PAPER 1

Incidence-angle dependence in forested and non-forested areas in Seasat SAR data

In: International Journal of Remote Sensing 1990.
Vol. 11, No. 7, pp. 1267–1276.

INT. J. REMOTE SENSING, 1990, VOL. 11, NO. 7, 1267–1276

Incidence-angle dependence in forested and non-forested areas in Seasat SAR data

YRJÖ RAUSTE

Technical Research Centre of Finland, Itatuulentie 2 A,
SF-02100 Espoo, Finland

Abstract. A major part of the variation in a Seasat SAR scene originates from terrain topography. Quantitative evaluation of the topography-induced variation was carried out. Differences in the slope of backscatter curve (sensitivity of radar to changes in incidence angle) between spruce-dominated mixed forests, pine-dominated mixed forests, deciduous forests and regenerated (pine plantations) areas were determined. Contribution of the corner reflector backscatter mechanism (a radar pulse is reflected from ground and tree trunks back to radar) to the total backscatter was evaluated.

Results of the analysis showed that:

65 per cent of the total variation in land pixels can be attributed to terrain topography;

Differences in the slope of backscatter curve were found to be significant (at 0·05 significance level) between spruce-dominated mixed forests, pine-dominated mixed forests, deciduous forests, and regenerated (pine plantations) areas;

The corner reflector backscatter mechanism does not constitute a significant part in the backscatter in the test site, where the ground surface (till) is relatively rough in terms of the radar wavelength.

1. Introduction

The application of microwave remote-sensing techniques in forestry applications has been studied for more than two decades (Morain and Simonett 1967, Sieber 1985, Teillet *et al.* 1985, Hoekman 1985, Hirosawa *et al.* 1987, Mougin *et al.* 1987, Westman and Paris 1987). Although the dominance of topographic effects has been identified as a limiting factor in the interpretation of synthetic-aperture radar (SAR) images of forests (Drieman 1987), only a few attempts have been made to evaluate the topography-induced variation in SAR images in quantitative terms (Foody 1986).

The spectral signature of an object can be defined as the reflectance of the object as a function of wavelength. By analogy, the angular (radar) signature of an object is defined as the backscattering coefficient of the object as a function of incidence angle. The incidence angle is defined as the angle between the surface normal and the direction of illumination by radar. Different forest types have different angular radar signatures due to different canopy structures and different surface roughness. Scattering from thick forest canopies is dominated by diffuse scattering, so the backscattering coefficient depends only slightly on incidence angle. In clear-cut areas, the specular scattering also contributes to the total backscatter. As a consequence, the backscattering coefficient drops with increasing incidence angle and so the slope of the backscatter curve is steeper. If a classification algorithm makes use of a known incidence angle, computed from an existing digital elevation model (DEM), it is essential to know at which incidence angle the backscatter curves cross each other.

Corner reflector backscattering or soil–trunk reflection occurs when a radar pulse is reflected by the soil surface to tree trunks and from trunks back to radar or *vice*

versa. The combination of soil surface and tree trunk, which are at right angles to each other, functions as a corner reflector. Corner reflector backscattering may in some cases be the dominant backscattering contribution (Ulaby *et al.* 1982, Richards *et al.* 1987, Sun and Simonett 1988 a,b).

The objectives of this study are to assess the impact of strong topographic effects on classification algorithms, to study differences in angular signatures of various types of forest cover, and to assess the significance of corner-reflector scattering. The ultimate goal of the study is to develop a computer-based interpretation algorithm making explicit use of known terrain topography.

2. Test site and data

The area covered by the digital elevation model and SAR data consists of mixed forests (mainly pine dominated), pine and spruce plantations, clear-cut areas, marshes and bodies of water. The tree-stem volume of forest varies typically between zero and about $100\,m^3\,ha^{-1}$ (not measured). In this area, spruce-dominated mixed forest usually has the densest canopy and the largest stem volume per hectare. Pine-dominated forest has the second largest stem volume per hectare and deciduous forest has the smallest. The height of the tallest trees varies typically between 10 and 15 m. The lower end of the crown in the tallest pine trees is usually four or five metres above ground. There are very few houses in the test site. Agricultural fields are present in only one spot in the area. Soil is predominantly till with some boulders. The diameter of these boulders seldom exceeds 50 cm. The terrain elevation varies between 420 and 780 m above mean sea level.

The SAR image data consists of a Seasat scene acquired on 20 August 1978. The wavelength of the Seasat SAR is 23 cm (L-band). The image, centred at 66·0°N, 17·3°E, covers an area of about 42 km by 40 km near the village of Arjepolog in Northern Sweden (figure 1). The image has a resolution of 25 m with four looks. In the SAR processing (processing of the raw SAR signal to an image, done by FOA 3 in Linköping, Sweden) a pixel size of approximately 16 m (in ground range) was used. The Landsat thematic mapper image, used as a reference, is quadrant number 2 (north-east) of scene 197-14 acquired on 25 June 1986.

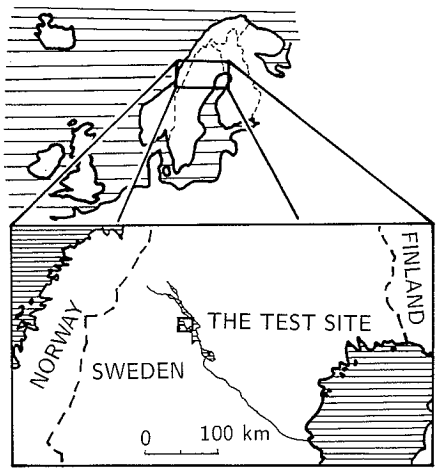

Figure 1. Location of the test site in northern Sweden.

The digital elevation model was generated by digitizing contours of a Swedish 1:100 000 topographic map. The digital elevation model covers an area of about 19 km (north) by 21 km (east) with a cell size of 25 m. The digital elevation model was generated by the Institute for Image Processing and Computer Graphics, Graz Research Centre, Graz, Austria. The SAR image was geocoded using the digital elevation model and a polynomial rectification method (Rauste 1988 a).

3. Methods of analysis

3.1. *Quantitative analysis of topographic effects in SAR data*

Linear regression was used to quantify the topographic effects on backscatter. In these analyses, the digital number in the SAR image was the dependent variable. The form of regression function is the sum of independent variables (each multiplied by its regression coefficient) and a constant term. A set of independent variables was computed for each pixel: simulated SAR image; stem volume per hectare; area of resolution cell; slope angle; and aspect angle.

The simulated SAR image was computed using a digital elevation model. A reference backscatter curve was generated by modelling the backscattering coefficient of land pixels with a second-degree polynomial of the incidence angle (Rauste 1988 b). This modelling was done by dividing each digital number of the Seasat SAR image by the area of the resolution cell and then generating a two-dimensional histogram (or scatter plot) of the backscattering coefficient against the incidence angle. In the simulation stage, the reference backscatter curve was used to assign an output value based on the pixel's incidence angle. This value was then multiplied by the area of the resolution cell.

The noise floor was subtracted from the SAR data before the modelling and simulation. Estimation of the noise floor was based on the darkest water areas in the image. Analysis of the digital elevation model showed that there were no radar shadows in the SAR image.

Stem volume per hectare was estimated using Landsat thematic mapper data and a regression model developed by Tomppo (1986). The regression model was developed for forests in northern Finland using an extensive forest inventory data set. The histograms of the thematic mapper image were normalized to match those of the image for which the regression model was developed. The standard deviation of the regression model is $17{\cdot}8\ m^3\ ha^{-1}$. The accuracy of the model for the test site is poorer than for the original scene, but the spatial variation of the estimated stem volume seemed to fit the real situation as checked visually on site.

The area of the resolution cell, slope angle and aspect angle (figure 2 (*a*)) were computed using the digital elevation model. The slope angle is defined as the angle between the plane of the surface element and a horizontal plane. The aspect angle is defined as the angle between the vertical plane containing the sensor and the centre of the surface element and the vertical plane in the direction of steepest slope of the surface element. The aspect angle is measured clockwise.

Speckle reduction was applied to SAR data prior to regression analysis. In the rectification of the SAR data, a weight function was used in which the weight fades to zero at six (input) pixels from the centre of the output pixel. Then pixel spacing of the image was reduced to 75 m by averaging over a window of 3×3 pixels.

The coefficient of determination (Robinson 1981) was used as a measure of the topographic effects. The coefficient of determination is defined as the variance

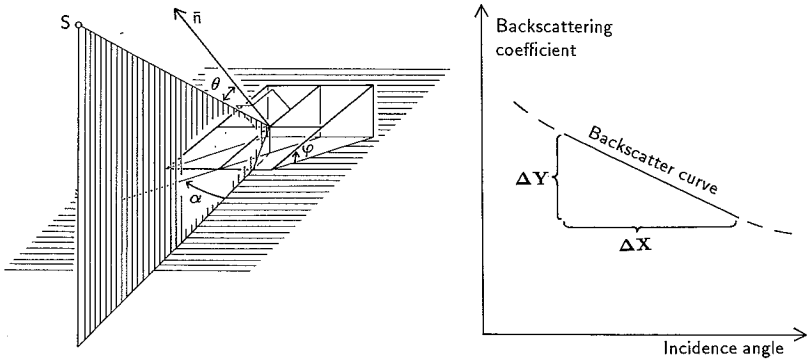

Figure 2. Definition of angles. Incidence angle θ, slope angle φ, aspect angle α, and the slope of the backscatter curve $\Delta y/\Delta x$.

accounted for by the linear regression model divided by the total variance of the dependent variable.

3.2. *Analysis of differences in incidence-angle dependence between forested and non-forested areas*

A two-dimensional histogram (scatter plot of the backscattering coefficient against the incidence angle) was generated for the following forest cover classes: spruce-dominated mixed forest; pine-dominated mixed forest; deciduous forest; and regenerated area.

A two-dimensional histogram (for all forest classes combined) is shown in figure 4. The classes were obtained by maximum likelihood classification of Landsat thematic mapper data. Border pixels (pixels adjacent to water or other non-forested areas) were excluded from the classification result. Starting with the two-dimensional histograms, a linear regression analysis was carried out using all the observations within the selected range of incidence angles (from 20° to 30°). Differences in the slopes of the regression lines (figure 2(*b*)) were tested using the test statistic (Hines and Montgomery 1980, p. 289)

$$t=\frac{x_1-x_2}{\left(\frac{s_1^2}{n_1}+\frac{s_2^2}{n_2}\right)^{1/2}} \tag{1}$$

where x_1 is the slope of the backscatter curve of the first forest cover class, x_2 is the slope of the backscatter curve of the second forest cover class, s_1 is the standard deviation of x_1, s_2 is the standard deviation of x_2, n_1 is the number of observations in the first forest cover class, and n_2 is the number of observations in the second forest cover class.

In the generation of the two-dimensional histograms, each pixel value was divided by the square root (amplitude image) of the area of the resolution cell. Therefore, the ordinate of the histograms is proportional to the square root of the backscattering coefficient. The abscissa is proportional to the cosine of incidence angle.

3.3. *Evaluation of the corner-reflector effect in forests.*

The backscattering from sparse forest canopies can be expressed as a sum of three components: direct backscattering from the vegetation; direct scattering from the soil; and multiply-reflected forward scattering involving both the soil and the vegetation (Ulaby *et al.* 1982, p. 865). The third component is strongest when tree trunks are at right angles to the ground surface (i.e. in flat areas).

It is assumed that the magnitude of this component drops rapidly when the angle between the tree trunks and the ground deviates from a right angle. Under this assumption, the backscattering coefficient of a uniform forest should be much higher for flat areas than for slopes. To test the presence of the corner-reflector effect, a simple experiment was carried out. The data was divided into two groups:

(*a*) flat pixels, where the surface normal deviated from the local vertical by less than 2°; and
(*b*) slope pixels, where the surface normal deviated from the local vertical more than 2°, but less than 5°.

The average slope was 1·2° in the flat group and 3·4° in the non-flat group. If it is assumed that this difference could cause a drop of 6 dB in the corner-reflector component and if this component dominated the backscatter, the expected backscatter (in an amplitude image) in the non-flat group should be about half that of the backscatter of the flat group.

Average backscattering coefficient and its standard deviation were computed for the flat and non-flat group. The difference in backscattering coefficients was tested using the test statistic (1). This test was carried out separately for spruce-dominated mixed forest, pine-dominated mixed forest, deciduous forest, and all forests combined.

4. Results

4.1. *Topographic effects in Seasat SAR data*

The number of observations (pixels) in the regression analyses was 23 446. Six cases were analysed. The independent variables in these analyses were simulated SAR data and stem volume, simulated SAR data only, stem volume only, area of resolution cell and stem volume, area of resolution cell only, and slope and aspect angles.

The results are shown in table 1. The correlation is significant in all six cases. The

Table 1. Regression analysis: SAR versus topography (=simulated SAR) and stem volume.

	Coefficient of determination (in per cent)	Correlation coefficient	F-ratio
Topography + Stem volume	65·4	0·808	22 121
Topography only	63·1	0·795	40 155
Stem volume only	0·3	0·052	64·3
Pixel area + Stem volume	62·4	0·790	19 469
Pixel area only	60·8	0·780	36 430
Slope + aspect	3·4	0·185	408

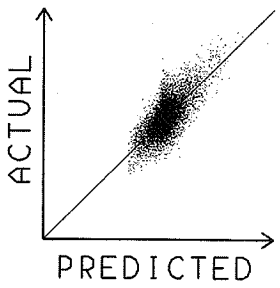

Figure 3. Residual errors of the regression: SAR digital number versus simulated SAR (topography) and stem volume.

aspect angle was the only single variable that did not contribute significantly to the correlation (the computed *t*-statistic was 0·09 while the critical value at 0·05 significance level is 2·0).

Figure 3 shows the residual errors when actual SAR data is regressed against simulated SAR data (topography) and stem volume. As can be seen, there is no need for higher-order polynomials in the regression.

The terrain topography is clearly the greatest constituent in the total variation of the SAR data. The stem volume alone, which is approximately proportional to the total biomass of the forest, could explain only 0·3 per cent of the total variance. Though the correlation was statistically significant using a sample of 23 446 observations, the correlation coefficient was very low. On the other hand, taking into account the stem volume improved the coefficient of determination by 2·3 percentage points (from 63·1 to 65·4) when used in conjunction with terrain topography. Thus, if the topography is not accounted for, it masks out most of the forest-canopy-induced variation in backscatter.

The residuals of the second regression (SAR data against the simulated SAR) were displayed in image form. Because the residual pattern is rather random, and because it does not conform to vegetation changes in the TM classification, it is probable that at least a part of the residual variance is due to small-scale topography, which is not depicted in the contour lines of a 1:100 000 topographic map. Therefore, the value of 63·1 per cent should be considered as a lower bound of the topographic effects (in an area like the test site).

The area of the resolution cell can explain almost as large a part (60·8 per cent) of the total variance as the simulated SAR (63·1 per cent). Because variation in the area

Table 2. Slope of the regression line: SAR versus incidence angle for various land-cover types.

Land cover	Slope	Standard deviation of slope
Spruce-dominated	−0·19	0·03
Pine-dominated	−0·27	0·02
Deciduous	−0·34	0·02
Clear-cut	−0·35	0·02

Table 3. Test of separation of the slopes of regression lines: t statistic for pairwise tests.

	Spruce	Pine	Deciduous
Pine-dominated	86		
Deciduous	153	148	
Clear-cut	167	195	32

of a resolution cell depends only on the imaging geometry, and not on the wavelength, this variation will be present also in the data from the future ERS-1 satellite. However, the proportion of the total variance explained by the area of the resolution cell will be smaller due to increased vegetation-related variation in the C-band.

4.2. *Differences in incidence-angle dependence between forested and non-forested areas*

The slope of the linear regression line was used as a measure of the incidence-angle dependence of radar backscatter. The slopes of the regression lines (the square root of the backscattering coefficient as a linear function of the cosine of the incidence angle) are shown in table 2. Results from the tests of separation of the slopes are shown in table 3. A scatter plot with regression lines is shown in figure 4.

All differences between the slopes of regression lines are significant since the critical value for the t-statistic at 0·05 significance level is 1·96. The incidence-angle dependence is weakest in spruce-dominated mixed forests, which have the oldest trees and densest canopy. The incidence-angle dependence is strongest in clear-cut and regenerated areas where the canopy contribution to backscatter is minimal. The forest canopy has a relatively uniform backscatter level relative to ground backscatter, which depends strongly on incidence angle.

The separation of regression lines in figure 4 increases with increasing incidence angle. This is probably due to the fact that in the L-band, at low incidence angles, most of the backscatter comes from ground (Hoekman 1987) and only at higher incidence angles does the forest canopy contribute significantly to the backscatter. At low incidence angles, the relatively uniform ground component in each forest-cover class masks out the small differences in backscatter originating from the canopy.

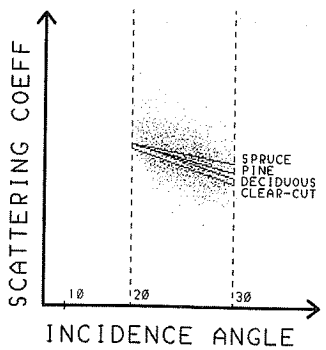

Figure 4. Regression lines adjusted to SAR versus incidence-angle data for spruce-dominated mixed forest, pine-dominated mixed forest, deciduous forest, and regenerated area.

Table 4. Average backscattering for flat and non-flat pixels. Arbitrary units, proportional to the square root of the backscattering coefficient.

	Flat	Non-flat
Spruce-dominated	104	107
Pine-dominated	102	107
Deciduous	105	105
Forests combined	104	106

4.3. *The corner-reflector effect in forests*

Table 4 shows average backscattering coefficients for flat (deviation from horizontal less than 2°) and non-flat (deviation from horizontal more than 2° but less than 5°) pixels for the following land-cover classes: spruce-dominated mixed forest, pine-dominated mixed forest, deciduous forest, and forest in general. Only pixels with incidence angle between 22·5° and 27° were included in the computation, to reduce the effect of incidence-angle change.

Because the average backscattering coefficient for flat pixels is always smaller than that for non-flat pixels, the corner-reflector effect seems not to dominate the backscattering from forest in the test site.

The average values of backscatter in table 4 are not directly comparable due to differences in the amount of stem volume per hectare (table 5). Table 6 shows the regression coefficient for stem volume for flat and non-flat pixels. The correlation (radar backscatter as a linear function of stem volume and terrain topography) was not significant for spruce-dominated flat areas. The regression coefficients are higher for non-flat areas (i.e. the dependence of radar backscatter on stem volume is higher on hill slopes than in flat areas). This phenomenon would be difficult to explain if the corner-reflector mechanism were the dominant component of backscatter in flat areas.

5. Discussion

The dependence of backscatter on terrain topography was high. The amount of variance accounted for by topography was 63·1 per cent. This is much higher than that determined by Foody (1986) for the airborne SAR-580 data, namely 5–25 per cent (with one exception of almost 50 per cent). The main reason for this difference is the difference in the method of analysis. The independent variables used by Foody

Table 5. Stem volume for flat and non-flat pixels ($m^3\,ha^{-1}$)

	Flat		Non-flat	
	Average	Standard deviation	Average	Standard deviation
Spruce-dominated	142	62	176	60
Pine-dominated	106	52	120	42
Deciduous	110	38	132	50
Forests combined	110	22	132	50

Table 6. Regression coefficient for stem volume for flat and non-flat pixels.

	Flat	Non-flat
Spruce-dominated	(0·044)	0·044
Pine-dominated	−0·039	0·058
Deciduous	0·060	0·109
Forests combined	0·020	0·087

(1986) were slope angle and aspect angle, which explained only 3 per cent of the total variance in the current study. If the main factor affecting radar backscatter is the area of resolution cell (60·8 per cent of the total variance), a linear combination of slope and aspect angles cannot be expected to explain the total variance well.

Sun and Simonett (1988 b) note that, at higher incidence angles, the volume scattering term tends to become dominant. Because this term is almost the same for many stands, it follows that discrimination between different forest stands is correspondingly reduced (at higher incidence angles). However, analysis of the incidence-angle dependence of forest-cover type showed that the separation between forest canopy types increases with increasing incidence angle. This was also confirmed using separability tests (Rauste 1988 b). The different behaviour of the discrimination capability as a function of the incidence angle comes from the fact that the trunk–ground term was insignificant in the test site of the current study and, consequently, it could not improve the discrimination capability at low incidence angles. Use of the increased discrimination power due to the tree–ground term at lower incidence angles in applications is complicated because variation in soils and small-scale topography affect this term strongly.

It was shown that the corner-reflector mechanism (or tree–ground term) does not contribute significantly to the backscatter in the test site. Richards *et al.* (1987) and Sun and Simonett (1988 a,b) proved that this term is the dominant contributor to the backscatter. The main reason for this difference is probably the ground surface. In the test site of this study, the prevalent soil is till (glacial drift) with stones and boulders of up to 50 cm diameter. This surface is rather rough, even in L-band wavelengths (23 cm). The underlying surfaces studied by Sun and Simonett (1988 a,b) were very level. Other factors decreasing the trunk–ground term in this study were low tree height and the branched canopy.

Acknowledgments

The study reported in this paper is part of the project SLARSAR funded mainly by the Technical Research Centre of Finland as a part of the research programme of space technology. In its earlier stages, the project has received support from the Academy of Finland and Nesté Ltd.

References

DRIEMAN, J. A., 1987, Evaluation of SIR-B imagery for monitoring forest depletion and regeneration in western Alberta. *Canadian Journal of Remote Sensing*, **13**, 19–25.

FOODY, G. M., 1986, An assessment of the topographic effects on SAR image tone. *Canadian Journal of Remote Sensing*, **12**, 124–132.

HINES, W. W., and MONTGOMERY, D. C., 1980, *Probability and Statistics in Engineering and Management Sciences*, 2nd edn (New York: John Wiley).

HIROSAWA, H., MATSUZAKA, Y., DAITO, M., and NAKAMURA, H., 1987, Measurement of backscatter from conifers in the C and X bands. *International Journal of Remote Sensing,* **8,** 1687–1694.

HOEKMAN, D. H., 1985, Radar backscattering of forest stands. *International Journal of Remote Sensing,* **6,** 325–343.

HOEKMAN, D. H., 1987, Multiband-scatterometer data analysis of forests. *International Journal of Remote Sensing,* **8,** 1695–1707.

MORAIN, S. A., and SIMONETT, D. S., 1967, K-band radar in vegetation mapping. *Photogrammetric Engineering,* **33,** 730–740.

MOUGIN, E., LE TOAN, T., LOPES, A., BORDERIES, P., and SARREMEJEAN, A., 1987, Backscattering measurements at X-band on young coniferous trees. *Proceedings of IGARSS'87 Symposium, held in Ann Arbor, Michigan, on 18–21 May 1987,* edited by M. C. Dobson (New York: I.E.E.E.) pp. 287–292.

RAUSTE, Y., 1988 a, Rectification of spaceborne SAR images using polynomial rectification and a digital elevation model. *Photogrammetric Journal of Finland,* **11,** 53–67.

RAUSTE, Y., 1988 b. DEM-based image processing methods for SAR images. *International Archives of Photogrammetry and Remote Sensing,* **27,** Part B3, Commission III, 696–705.

RICHARDS, J., SUN, G., and SIMONETT, D. S., 1987, L-band radar backscatter modeling of forest stands. *I.E.E.E. Transactions on Geoscience and Remote Sensing,* **25,** 487–498.

ROBINSON, E. A., 1981, *Least Squares Regression Analysis in Terms of Linear Algebra* (Houston, Texas: Goose Pond Press).

SIEBER, A. J., 1985, Forest signatures in imaging and non-imaging microwave scatterometer data. *E.S.A. Journal,* **9,** 431–448.

SUN, G., and SIMONETT, D. S., 1988 a, Simulation of L-band and HH microwave backscattering from coniferous forest stands. A comparison with SIR-B data. *International Journal of Remote Sensing,* **9,** 907–925.

SUN, G., and SIMONETT, D. S., 1988 b, A composite L-band HH radar backscattering model for coniferous forest stands. *Photogrammetric Engineering and Remote Sensing,* **54,** 1195–1201.

TEILLET, P. M., GUINDON, B., MEUNIER, J.-F., and GOODENOUGH, D. G., 1985, Slope-aspect effects in synthetic aperture radar imagery. *Canadian Journal of Remote Sensing,* **11,** 39–49.

TOMPPO, E., 1986, Stand delineation and estimation of stand variates by means of satellite images. *Proceedings of the Seminars on Remote Sensing-aided Forest Inventory held in Hyytiälä, Finland, on 10–12 December 1986. Helsingin Yliopiston metsänarvioimistieteen laitoksen tiedonantoja* No 19 (Research Notes No. 19) (Helsinki: University of Helsinki, Department of Forest Mensuration and Management), pp. 59–76.

ULABY, F. T., MOORE, R. K., and FUNG, A. K., 1982, *Microwave Remote Sensing, Active and Passive,* Vol. II (Reading, Massachusetts: Addison Wesley).

WESTMAN, W. E., and PARIS, J. F., 1987, Detecting forest structure and biomass with C-band multipolarization radar: physical model and field tests. *Remote Sensing of Environment,* **22,** 249–269.